Validation of DTI-tractography-based measures of white matter pathways originating from the primary motor area

Yurui Gao[1,2], Ann S. Choe[1,2], Xia Li[1], Iwona Stepniewska[3], and Adam W. Anderson[1,4]

[1]VUIIS, Vanderbilt University, Nashville, TN, United States, [2]BME, Vanderbilt University, Nashville, TN, United States, [3]Psychology, Vanderbilt University, Nashville, TN, United States, [4]BME, Radiology and Radiological Science, Vanderbilt University, Nashville, TN, United States

INTRODUCTION

In our previous study [1], we validated DTI-tractography-based measures of primary motor area (M1) cortical-cortical (C-C) connectivity. To further understand our previous validation result, in this study we investigated the agreement between DTI-tractography-derived white matter pathways and histological pathways. We reconstructed the 3D pathway of histological fibers as well as DTI fibers originating from the M1 forelimb subarea in the squirrel monkey and then quantitatively measured the agreement between these two pathways. We also describe potential reasons for the failure of DTI tractography to align perfectly with histological tracts.

MATERIALS AND METHODS

Data acquisition: The bidirectional neural tracer biotinylated dextran amine (BDA) was injected into 8 sites covering the forelimb movement representation area in the left M1 cortex of the monkey. After two weeks, the brain was extracted, fixed and scanned using a 9.4T Varian scanner (PGSE, TR=4.6s, TE=42ms, gradient directions=32, b=1022s/mm^2, voxel size=0.3mm×0.3mm×0.3mm, data matrix=128×128×192). Then the brain was sectioned in coronal planes at 50μm thickness on a freezing microtome and the blockface was photographed for every third section. Every sixth section was reacted for BDA (each adjacent section was stained for myelin) and photographed under a light microscope (0.5 X and 1.25 X objectives).

Data processing: BDA-stained white matter fibers were automatically segmented by morphological techniques on 1.25X micrographs. Using computer-assisted gridding and counting, a density map (256×256) of BDA-stained fibers was produced. The density maps were transferred from the micrograph space to the DTI space using deformation fields calculated via a thin-plate spline algorithm to register each BDA micrograph to the corresponding blockface image and the adaptive bases algorithm [2] to register the blockface volume to the DTI volume. A surface enclosing the occupied volume of BDA-stained fibers was reconstructed by extracting the isosurface from the transformed 3D density map in DTI space.

DTIStudio[3][4] was used to perform deterministic fiber tracking (stop FA=0.2, stop angle=70° , denoted by 'DS' scheme) using the transformed BDA injection region as the seed region. The DTI fiber density map was produced by counting the DTI fibers passing through every DTI voxel. FSL [5] was used to produce a density map of probabilistic fibers with the same seed region. The ARD weight in FSL was assigned to 1 and 0.5 respectively (denoted by 'FSL1' and 'FSL2' schemes). Seed regions at three depths in the white matter (denoted by 'dw') were used for the above three schemes. Additionally, the injection region in micrograph space was manually segmented based on architectonics of BDA-stained and Nissl-stained neurons [6].

Data analysis: To indicate the general agreement between histological white matter pathways and DTI-derived pathways, we calculated the agreement coefficient: $AC = \frac{2(V_B \cap V_D)}{V_B + V_D}$, where V_B(or V_D)is the density-weighted BDA (DTI) volume. The density-weighted agreement coefficient provides a more realistic estimate of agreement than a simple measurement of volume overlap [7].

RESULTS

Figure 1 displays the volume of BDA-stained fibers overlaid respectively by the DS fibers and volume occupied by FSL fibers (FSL1 and FSL2) rendered within the external surface of gray matter. Table 1 shows the agreement coefficient for each tractography scheme using different dw. Figure 2 illustrates an example of BDA-stained fibers, myelin-stained fibers and DS tensor within the same voxel (0.3mm×0.3mm).

CONCLUSION AND DISCUSSION

Visual comparison of fiber-occupied volumes in Fig. 1 shows that the three tractography schemes produced false positive (FP) and false negative (FN) white matter pathways, which might lead to the FP and FN result for measures of C-C connectivity in [1]. Comparison of the agreement coefficients for different tractography methods in Tab. 1 indicates that probabilistic tractography has the potential to provide white matter pathways with better agreement with histology than deterministic tractography does. In addition, agreement coefficient increases as the dw of the seed region increases, which is also consistent with [1]. One of the reasons for DTI tractography to disagree with BDA fibers is illustrated in Fig. 2. The diffusion tensor in Fig. 2d tends to characterize the superior-to-inferior orientation corresponding to major myelinated fibers shown in Fig. 2c in the voxel. When major BDA-stained fibers running from left to right in Fig. 2b are a minority of the whole fiber population in that voxel, it will be hard for DTI tractography to follow the left-to-right fiber bundle.

REFERENCES

1. Gao, ISMRM, 2011. 2. Rohde, IEEE Trans Med Imaging, 2003. 3. Mori, Ann Neurol, 1999. 4. Jiang, Comput Methods Programs Biomed, 2006. 5. Behrens, Neuroimage, 2007. 6. Stepsnewska, J Comp Neurol, 1993. 7. Dauguet, Neuroimage, 2007.

	dw		
	0mm	0.3mm	0.6mm
DS	0.55	0.62	0.67
FSL1	0.62	0.68	0.71
FSL2	0.71	0.78	0.81

Tab.1: Agreement coefficients (AC) of three tractography schemes (in rows) using seed region with three depths into white matter (in columns)

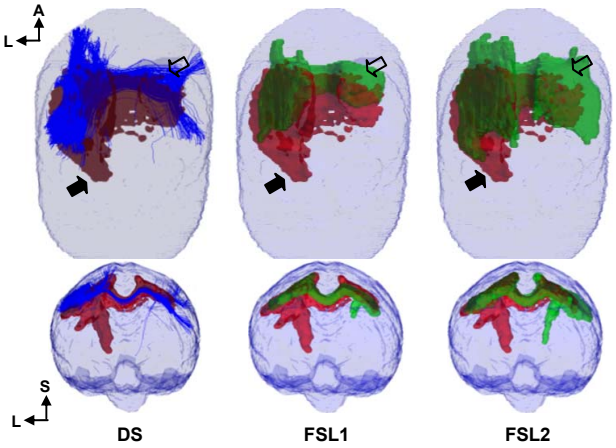

Fig.1. Dorsal and frontal view of occupied volume of BDA-stained fibers (red volume) overlaid on the DS fibers (blue lines in first column), occupied volume of FSL fibers (green volume in last two columns). False negative and positive results are highlighted by the solid and empty arrows, respectively.

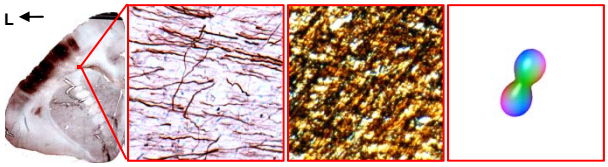

Fig.2. Example of BDA-stained fibers (b), myelin-stained fibers (c) and diffusion tensor (d) within the same voxel located at (a) the left hemisphere far under the premotor cortex.